Shock Wave Science and Technology Reference Library, Vol. 5

Non-Shock Initiation of Explosives

Bearbeitet von
Blaine Asay

1st Edition. 2010. Buch. XVIII, 618 S. Hardcover
ISBN 978 3 540 87952 7
Format (B x L): 15,5 x 23,5 cm
Gewicht: 1221 g

2

Transport Phenomena for Nonshock Initiation Processes

W. Lee Perry

2.1 An Overview of Transport Theory in Explosives Problems

A useful explosive material is, of course, stable under reasonable environmental conditions. It will neither release energy nor produce gas without some kind of thermal stimulus. The possible stimuli include impact, spark, friction, boundary heat, or shock. These processes raise the temperature of the explosive material, either in a localized volume, or throughout its entire volume, to a point where the exothermic, gas-producing reaction becomes self-sustaining (ignition). We refer to the events leading to self-sustaining reaction as the preignition regime, and the behavior after self-sustaining reaction commences as the post-ignition regime. We further generally characterize the post ignition regime by either laminar nonviolent deflagration; violent, convectively driven explosion; or the process may undergo a transition to detonation (DDT).

Transport phenomena are inherent to the nonshock initiation process and post-ignition behavior. Specifically, transport phenomena are the movement of heat (energy), molecular species, and momentum under the influence of temperature, species concentration, pressure, and velocity gradients. The theory of these phenomena, together with the production of gas and heat from chemical reactions (kinetics and thermodynamics), in principle fully describe the processes that occur prior to ignition (preignition) and what happens after (post-ignition). In practice, the theory has only been applied to very simple situations due to the complexity of the integrated problem.

The stimuli listed above all serve to raise the temperature of the explosive either within a volume small with respect to the charge (impact, spark, friction, shock) or globally (boundary heat). Each of these stimuli will be discussed in detail in other chapters of this text. As these are the initial drivers for the ignition process, we briefly introduce them here. Impact leads to localized heating when deformation becomes concentrated, where the material fails by cracking, or when the yield strength is exceeded and causes shear localization and concentration of energy along shear bands (Chap. 10). Spark energy

B.W. Asay (ed.), *Shock Wave Science and Technology Reference Library Vol. 5: Non-Shock Initiation of Explosives*, DOI 10.1007/978-3-540-87953-4_2,

is localized along the spark channel (Chap. 11). Friction (Chap. 9) localizes heat between moving surfaces or at specific locations, where, for example, foreign matter (grit) becomes trapped between the surfaces (the latter has been implicated in accidents.) A shock wave compresses material along its leading edge and causes heat generation directly by adiabatic compression of the material itself, by collapsing void space, or by grain boundary interactions. Boundary heat, as the phrase implies, is heat applied to the outer surfaces of an explosive charge, or its container, and the most common source is fire, and ignition by this method is commonly called "cookoff" (Chap. 7).

Chapter 3 discusses reaction kinetics and thermodynamics. We mention them here in the context of heat transport because, of course, exothermic chemical reaction becomes the driving force for the ignition and combustion process once one (or more) of the ignition stimuli meet a critical criterion. To a first order, the general Arrhenius expression provides an illustration of the rate of gas production as a function of temperature and some reactive state, $f(X)$, of the explosive (e.g., reaction extent, density, concentration of reactive species, available surface area, etc.):

$$\dot{N} = A \cdot \exp\left(-\frac{E}{RT}\right) \cdot f(X). \tag{2.1}$$

The product of enthalpy change (per mole converted) and the rate of gas production reveal the rate of heat production:

$$\dot{Q} = \dot{N} \cdot \Delta h. \tag{2.2}$$

These expressions illustrate the sensitivity of the process to temperature in the exponential term and the dependence of some reactive state of the explosive. When one (or more) of the listed stimuli is applied with sufficient intensity to raise the temperature to a value where significant heat production occurs, ignition may occur. The specific ignition threshold is crossed when the rate of heat production in a volume exceeds the rate of heat removal from that volume by a heat transport process (conduction, convection, or radiation). For combustion to spread, energy must be fed back from the combustion zone to regions of unreacted material at a sufficient rate to maintain combustion. These are central concepts of ignition and propagation theory and will be discussed throughout the book. As described, ignition and reaction spread arise from the specific interplay of heat transport behavior, reaction kinetics, and the thermodynamics of the involved reactions.

Heat transport theory has played a central role in determining the factors that lead to ignition. The critical conditions for ignition are determined by applying the principle of energy conservation on the stimulated volume, balancing heat production by chemical reaction and heat loss by conduction or convection. In conjunction with carefully constructed experiments, the application of heat transport theory has also provided a tool to help deduce

or verify the specific chemical steps that occur in the preignition regime [1]. Heat transport theory is also well-developed in the post-ignition regime for low-order (nonviolent) laminar combustion of simple regressing solid or liquid surfaces where heat feeds back from the combustion zone to the surface liberating the reactive species [2, 3]. However, for cases of more critical interest where violent explosive reaction occurs, heat transport occurs in a very dynamic, multidimensional, multiphase environment. Although the basic processes and theory are fairly well understood, the complexity challenges our best computational tools and this remains a very active area of research.

Species transport is the movement of specific chemical constituents throughout a system. Explosives considered in this text generally consist of a single molecular constituent. In the preignition regime, the aforementioned stimuli can cause direct decomposition to combustion products, decomposition to intermediate species, or sublimation/evaporation of the original substance. In each of these cases, species transport phenomena govern the physical movement of the products or sublimated species from a solid or liquid surface into the gas phase. The rates of these processes and any associated exothermicity are again controlled by kinetics, which of course is strongly temperature dependent, but also dependent on species distributions and/or morphology ($f(X)$). If the explosive is heterogeneous (e.g., HMX powder), species transport governs how the gas phase species will distribute themselves throughout pre-existing void space, or throughout the void space created by decomposition, sublimation, phase changes, etc. (mechanical or thermal damage). Recent research has concluded that the void space (pore structure) and its potential development and spatial distribution prior to ignition has a very significant effect on the post-ignition behavior (Chap. 6) [4].

The distribution of species, whether in homo- or heterogeneous system, determines, in part, $f(X)$ in (2.1) above and therefore affects the preignition heat transport behavior. Recent work has shown this distribution of reactive species affects the temperature distribution [5]. This in turn affects the post-ignition spread of combustion from the ignition locus as it propagates into a larger volume at a higher temperature and in a more reactive state [6]. Further, combustion spreads more readily into regions previously saturated with combustible species. As with heat transport, the situation during violent explosive reaction becomes exceedingly complex, and to date, no significant computational work has been done, which includes rigorous species transport in the post-ignition regime. In the post-ignition regime, species transport theory has also been applied to the study of laminar flames where convection and diffusion processes carry reactive species into the combustion zone [7, 8].

Heat production, decomposition, combustion, and sublimation/evaporation all potentially lead to pressure gradients, which are the driving force for momentum transport. Momentum transport is responsible for the convective (advective) movement of both heat and species. In the pre-ignition regime, localized heating from impact, spark, or friction leads to local gas formation by decomposition or sublimation, causing a local region of elevated pressure

relative to the bulk of the explosive. In the case of boundary heating, the evolving temperature profiles will cause a distribution of gas products and a resulting pressure distribution. In both these cases, the pressure gradients cause the transport of momentum, which carry heat and species, affecting pre- and post-ignition behavior as already described.

The rigorous incorporation of momentum transport requires the Navier–Stokes (NS) equations, which for any practical problem require the art of Computational Fluid Dynamics (CFD). The tensorial nature of the NS equations and the presence of multiple phases add a large degree of complexity to an already exceedingly complex problem and have not been applied in the preignition regime. However, the porosity and permeability of some explosives have been determined [9, 10], and it was suggested that Darcy's law for permeation in porous materials would provide a tractable means to incorporate momentum transport for analysis of the preignition problem [5, 11]. This approximation has provided good insight to the preignition problem and allows models to correctly predict temperature profiles for a boundary-heated system [5]. The Darcy's law approximation requires low Reynold's number flow, which of course is not the case for the violent post-ignition regime. In that regime, high flow rates in stationary media occurs in the initial phases; as momentum is transferred to the solid phase and the pressure builds, the solid phase disassembles and is set in motion by drag forces. In this complex multiphase flow regime the full NS system is required. These have not been incorporated into contemporary computational solutions; however, progress has been made in formally formulating the problem and examining tractable limiting cases [9]. For the most violent possible post-ignition outcome, DDT, multiphase momentum transport also governs the formation of compaction waves that build to a shock wave and initiate the shock-to-detonation transition (SDT) [12]. Although our understanding of the mechanism of DDT is fairly mature (Chap. 8) [13], only a limited amount of work has been done to apply formal momentum transport theory to the problem.

Hopefully, this brief introduction has given the reader a flavor of the interconnection of the three transport modes through heat and mass production by chemical reaction and the importance of all three modes to the ignition and explosion behavior. In the rest of this chapter, we will provide an overview of the history of the application of heat transport theory to explosive systems. We will then introduce the fundamental equations of heat transport theory as an introduction to other chapters that provide a more complete development. Properties such as heat capacity, thermal conductivity, viscosity, etc. are crucial to accurate transport theory predictions, and so a section will be devoted to that topic. Finally, we will conclude the chapter with an overview of three recent problems that employ formal transport theory in a way that has enhanced our physical understanding of the ignition and combustion process.

2.2 The Origins of Transport Theory in the Field on Nonshock Initiation

In our modern world of advanced computing tools, we may lose sight of the fundamental transport processes involved in the nonshock initiation and combustion of explosives. The early work in this field, prior to the existence of modern computing tools, required very insightful analysis and therefore deserves a brief review. Explosion is merely an extreme form of flame propagation, such that early flame research provides a logical origin of transport theory development for ignition and combustion of explosives. Scientists have known for over 150 years that combustion and flame propagation involved the transport of momentum, chemical species, and heat. This is evident in the lively and engaging compilation of lectures by Michael Faraday entitled *The Chemical History of a Candle*, published in 1861 [14]. Early theory of flame propagation velocity was published by Ernest-Francios Mallard in 1875 [15], and further developed by both Mallard and the famous physical chemist Henry Le Chatelier [16]. The Nobel Prize winning Dutch physical chemist Jacobus van't Hoff provided early insight in the late nineteenth century to the nonequilibrium nature of combustion by suggesting that an exothermically reacting system cannot be in equilibrium with its surroundings [17]. The early development of transport theory for combustion and ignition of energetic materials mostly belongs to the Russians. In the 1920s and 1930s, Yakov Zeldovich [18, 19] and Belyaev [20] pioneered the early application of transport theory to the combustion of gasses and solid energetic materials.

In the same time period, Todes and Seminov provided the earliest recognized formal heat transport theory of the critical conditions for the initiation of thermal explosion for a boundary-heated system [21, 22]. Seminov's unsteady treatment is widely cited and discussed today and is distinguished by its simplicity, qualitative nature, and illumination of physical features important to criticality. His analysis showed the conditions for which heat production exceeded heat removal, the condition for ignition, using simplified mathematics. To find an analytical solution, Seminov included an exponential temperature-dependent reaction term, but neglected heat transport within the explosive material, that is, the spatial derivatives, such that all resistance to heat transfer occurred at the material's surface. However, it was known experimentally at the time that ignition generally occurred at a specific location within the explosive material, implying that an accurate analysis could not neglect internal heat transport. David Frank-Kamenetskii, a student of Seminov, took a different approach from his mentor and developed a steady-state solution that included internal heat conduction (spatial derivatives) and also included the nonlinear reaction term [23]. An essential feature of Frank-Kamenetskii's analysis was the use of Seminov's steady-state solution to develop a dimensionless temperature having a value near 1 at the explosion temperature and zero initially. The interplay between the works of these two researchers continued, as it was later recognized that Frank-Kamenetskii's steady solution could

provide key parameter information for Seminov's unsteady solution such that a fairly clear picture of (transient) thermal explosion behavior emerged. When exactly this latter insight came about is unclear, but it is discussed in a text published by Frank-Kamenetskii in 1947 [24]. Their methods of solution and the results are especially clever and insightful considering the lack of computational resources. The work of these early researchers, embodied in the theories of Seminov and Frank-Kamenetskii, are essential for the understanding of energetic material ignition, primarily due to the clear presentation and illumination of salient features. As such, Chaps. 4 and 7 go into much greater detail of the development and predictive qualities of these theories.

This early development of ignition theory was concerned with the boundary heating problem; investigation of hot-spot heating followed soon after. It was recognized in the 1940s that the size of a hot spot played a role in the critical conditions for ignition. This idea may have originated from intuition stemming from knowledge of heat transport theory, cognizance of the size effect in the Frank-Kamenetskii/Seminov boundary analyses, or more likely, both. Bowden et al. confirmed this when they observed a size effect in friction experiments, the results of which were reported in 1947 [25]. This size effect was shown theoretically in 1948 by the hot-spot analysis of Rideal and Robertson that examined impact ignition [26]. In that study, the researchers formulated the one-dimensional spherical transient and spatially dependent heat transport problem and presented an analytical solution. The analytical solution was possible because they neglected the nonlinear exothermic reaction term and imposed a temperature, rather than a heat source term. They determined critical hot-spot volume and temperature by equating the rate of heat conduction at a given temperature and spot size to heat evolved from chemical reaction over the same volume. As with the early work on boundary-heated ignition, computational tools did not yet exist to provide numerical solutions to the nonlinear equations that govern the hot-spot problem. In fact, these authors admit: "A more elegant and satisfactory treatment, however, would be to solve the general equation. . .," referring to the unsteady 1D spherical heat equation with an Arrhenius heat generation term. Apparently, very little work was done on the hot-spot problem until the advent of numerical tools. In 1963, Merzhanov and his coworkers published the results of their numerical study that followed the dimensionless parameterization scheme of Frank-Kamenetskii [27]. They concluded that those parameters were also good indicators of criticality for the hot-spot ignition problem, although with a different functional dependency on temperature.

The usefulness of the Frank-Kamenetskii parameters for finding the properties of a critical hot spot arises due to the universal physical basis for criticality. While boundary heating may be generic in nature, specific localized mechanisms cause hot-spot heating. In those cases, an additional criterion is required: localized power dissipation from the heating mechanism must also exceed the rate of local cooling such that the hot spot will reach a critical temperature. A current good review was provided by John Field et al.

in 1992 [28]. They point out the important early contributions to impact and friction studies of Bowden et al. [25], Eirich and Tabor [29], Rideal and Robertson [26], Bowden and Yoffe [30], Afanas'ev and Bobolev [31], and Field and his coworkers [28]. Many of these studies are mechanistic in nature and some report a temperature rise under the stimulated conditions. From a transport theory perspective, it is most useful to have a rate of energy dissipation (power). Spark initiation studies provide a simpler platform to quantify energy and power from the electrical properties of the spark generator. Langevin and Bicquard published early studies of the spark initiation of primary explosives in 1934 [32]. Wyatt and his colleagues published their studies of spark initiation of primary materials in 1958 [33], and Tucker reported their research on secondary explosives in 1968 [34]. Somewhat surprisingly, these early papers, with some exceptions in spark initiation research, represent the state of the art of hot-spot ignition source research. Although mechanisms are fairly well understood, heat production in the context of transport theory has not been fully investigated and this remains an active area of research.

So far, we have reviewed the foundations of ignition theory and laminar (nonviolent) combustion. It was known in the late 1950s that sufficient pressure would cause an explosive deflagrating from its outer surface to transition to a violent thermal explosion as flame penetrated into the bulk via an existing pore network or cracking induced by pressure. It was also known in this period that this phenomenon, usually called "convective burning," was a critical step for DDT. In terms of transport phenomenon, this physical transition is reflected by the mathematical transition to theory where momentum transport analysis becomes essential for understanding the movement of heat and chemical species. The Englishmen Griffith and Groocock published their early work in 1960 [35], as did the contemporary Russian researchers Andreev and the already-mentioned pioneer Belyaev [36]. In 1962, Taylor published his work on the convective burning mechanism in HMX [37]. The evolution of this research was in part motivated by the potential for solid rocket motors, some of which were propelled by HMX and/or RDX, to explode or detonate under abnormal pressure conditions. As such, the propellant literature from the 1960s and 1970s provide the most complete theoretical transport basis for the convective burning problem and the review text of Kenneth Kuo and Martin Summerfield provides an excellent fundamental overview [38]. The process of DDT begins when the drag forces of moving gases become sufficient to set the solid phase into motion, thus amplifying the complexity of the problem. Bernecker and Price credited the aforementioned work of Griffiths and Groocock [35] in an early review in 1979 as providing the first complete description of DDT in a bed of granular explosive [39].

Perhaps it is not surprising that the theory of explosion originates coincidentally with the understanding of chemical equilibrium. The early contributions of the Russian researchers cannot be overstated, as followed by the English at Cambridge and, most recently, the researchers funded by the American Department of Defense. Over the last 20 years, researchers funded

by the US Department of Energy have pursued this area of research in order to understand and minimize the consequences of a nonshock initiation event in a nuclear weapon system. While the early research has provided a reasonably clear picture of mechanisms and the appropriate theory, the evolution of computational tools and their ever-increasing ability to incorporate nonlinear, multiphysics, multiphase phenomena at ever-increasing spatial and temporal resolution now drives the advancement of the field. However, one cannot build good models without the basic theory and insight. That is the intent of this book. To follow the evolution of these research topics beyond their origins, the reader may perform a citation search from this section, and the texts of Frank-Kamenetskii and Zeldovich provide a complete theoretical foundation of transport theory in explosive systems. The other chapters of this book will provide the details of the most recent research.

2.3 Physical Properties Used in Transport Theory Analysis

Solving the transport equations requires the physical properties including heat capacity, density, thermal conductivity, thermal diffusivity, viscosity, and species diffusion coefficient. These properties depend directly on the thermodynamic state of the system: pressure, temperature, etc. Common high performance explosives and explosive composites have well-characterized heat capacity, density, and thermal conductivity and data are available up to temperatures where decomposition reactions become significant. The reference text of Gibbs and Popalato [40] or the LLNL Explosives Handbook [41] provides these data for a wide range of explosives. For gases or liquids involved in the explosion process, viscosity and the diffusion coefficient also become factors. For tabulated data for all the properties for gases and liquids, except the diffusion coefficient, we refer the reader to general sources such as the CRC handbook [42] and the NIST Chemistry Web Book [43]. The diffusion coefficient depends on factors specific to the specific environment and tabulated data are sparse, but some data are provided in textbooks covering diffusion; See, for example, [44] and the references therein. Here we review the physical basis for each property, general value ranges, and general trends with pressure and temperature.

Specific Heat. In conjunction with density and molecular weight, specific heat (on a mole basis) provides a measure of the thermal inertia of a system. That is, it is a measure of the resistance of a system to a change in energy content (temperature.) As such, specific heat affects transient heat conduction, but has no effect on steady-state heat conduction. Specific heat is mathematically defined as

$$c = \left(\frac{\delta q}{\mathrm{d}T}\right)_{\text{path}}. \tag{2.3}$$

In order to make tractable relationships, the path is taken to be one of constant pressure or constant volume. For a constant volume process, specific heat is related to the internal energy:

$$c_{\mathrm{V}} = \left(\frac{\mathrm{d}u}{\mathrm{d}T}\right)_{\mathrm{V}}. \tag{2.4}$$

For a constant pressure process, the specific heat is related to enthalpy:

$$c_{\mathrm{p}} = \left(\frac{\mathrm{d}h}{\mathrm{d}T}\right)_{\mathrm{P}}. \tag{2.5}$$

For ideal gases, it can be shown that

$$c_{\mathrm{p}} - c_{\mathrm{v}} = R.$$

And the ratio of the specific heats commonly appears in gas-phase problems:

$$\gamma = \frac{c_{\mathrm{p}}}{c_{\mathrm{v}}}. \tag{2.6}$$

Due to the relative incompressibility of the solid and liquid states, $u = h$ such that

$$c_{\mathrm{p}} \approx c_{\mathrm{v}}.$$

A simple relationship exists for the internal energy stored by a single degree of freedom regardless of the size or shape of the molecule:

$$u = \frac{1}{2}RT. \tag{2.7}$$

And

$$c_{\mathrm{v}} = \left(\frac{\mathrm{d}u}{\mathrm{d}T}\right)_{\mathrm{v}} = \frac{n}{2}R \tag{2.8}$$

for n degrees of freedom. For example, monatomic gas molecules translate through three dimensions and therefore have three degrees of freedom, such that

$$c_{\mathrm{v}} = \frac{3}{2}R. \tag{2.9}$$

The presence of rotational, vibrational, torsional, etc. modes increases the heat capacity accordingly. The free electrons in conducting solids contribute to the heat capacity at room temperature on the order of $0.03R/2$. Not all modes are active at all temperatures and there are other temperature effects for more complex structures. The reader should consult a physical chemistry text or a statistical thermodynamics text for details of specific molecules and temperatures.

Monatomic gasses have a specific heat exactly $3R/2$ and diatomic gasses such as nitrogen, oxygen, carbon monoxide, etc., at room temperature are also near $3R/2$. Liquid water at room temperature is $75.9\,\mathrm{J\,mol^{-1}K^{-1}}$. Solid copper has a specific heat of $24.4\,\mathrm{J\,mol^{-1}K^{-1}}$ and the common organic crystalline explosive HMX has a specific heat of $325\,\mathrm{J\,mol^{-1}K^{-1}}$ at room temperature.

Density plays a role in all three transport processes. It affects the transient solution of the heat transport equations and both the transient and steady state solution of the momentum equations. For reasonable temperatures and pressures found in the preignition regime, gas phase density may be computed from the ideal gas law equation of state. In the more nonideal post ignition regime, a more descriptive equation of state, such as the van der Waals equation of state, may be required. In extreme post-ignition conditions, with pressures and temperatures approaching detonation conditions, an equation of state such as the Abel or Becker–Kistiatowsky–Wilson equation of state may be necessary.

Solid and liquid phase densities for preignition conditions are almost always measured quantities. Most liquids fall into the range of 800–1,200 $\mathrm{kg\,m^{-3}}$. Most inorganic solids have crystal densities in the range of 1,500–3,000 $\mathrm{kg\,m^{-3}}$. Most metals are in the range of 2,500–12,000 $\mathrm{kg\,m^{-3}}$, with exceptions that exceed 13,000 $\mathrm{kg\,m^{-3}}$ such as mercury, uranium, plutonium, etc. Common organic crystalline explosives and their binders have densities in the range of 1,500–2,000 $\mathrm{kg\,m^{-3}}$.

Thermal conductivity is the proportional factor of Fourier's Law of Heat Conduction, relating heat flux to a temperature gradient. As with density and heat capacity, thermal conductivity affects transient heat conduction. However, it also appears in the steady state solution. Gas thermal conductivity is related to the heat capacity of the particular molecule, the characteristic velocity, and the mean-free path. The kinetic theory of gases reasonably predicts the thermal conductivity of simple gases to 10 atm (or so) [45]:

$$k = \frac{1}{d^2}\sqrt{\frac{\kappa^3 T}{\pi^3 m}}, \tag{2.10}$$

where d is the molecular diameter, k is the Boltzmann's constant, and m is the mass of the molecule. This general expression shows that pressure has a weak overall effect on thermal conductivity. Thermal conductivity of gases is on the order of 0.01–0.05 $\mathrm{W\,m^{-1}K^{-1}}$, but can increase by a factor of 10 at combustion temperatures.

In liquids, thermal conductivity is roughly an order of magnitude greater than gases because of the shorter mean free path. The kinetic theory of gases provides a starting point that leads to

$$k \approx \pi^{2/3} d^2 v_\mathrm{s} = \pi^{2/3} d^2 \sqrt{\frac{C_\mathrm{p}}{C_\mathrm{v}}\left(\frac{\partial P}{\partial \rho}\right)_T}, \tag{2.11}$$

where v_s is the sound velocity. In most cases for liquids, the ratio of heat capacities is unity and the pressure–density relationship must be found from an appropriate equation of state. As such, liquid thermal conductivity also has a weak dependency on pressure, but no general temperature behavior. It may increase or decrease depending on the equation of state for the particular liquid. The thermal conductivity of liquids is on the order of 0.1–0.5 $\mathrm{W\,m^{-1}K^{-1}}$.

In solids, phonons and free electrons exchange momentum to cause heat conduction. For metallic solids, the dominant mechanism is the latter, and (2.10) above will provide an estimate and trends when evaluated for the electron gas. For non-metallic solids, phonon interaction (frequency) dominates and thermal conductivity generally increases with temperature. For non-metallic solids, conductivity ranges over 0.5–5, and metallic solids typically are on the order of hundreds of $\mathrm{W\,m^{-1}K^{-1}}$. Common organic explosives and their binders are in the range of 0.1–0.6 $\mathrm{W\,m^{-1}K^{-1}}$.

Thermal diffusivity is the ratio of the thermal conductivity to the product of density and heat capacity:

$$\alpha = \frac{k}{\rho c}. \tag{2.12}$$

It is a measure of the efficacy of conduction of thermal energy relative to the storage of thermal energy. This may be thought of as thermal inertia or the rate of diffusion of heat. Thermal diffusivity always appears in the exponential terms of the transient solution of heat transport analyses; large values reflect short transients. The dimensionless Fourier number provides an estimate of the thermal time constant of a system when its value is near unity:

$$\mathrm{Fo_c} = \frac{\alpha\tau}{L^2} \approx 1, \tag{2.13}$$

where L is a characteristic length. Simple gases at STP have a thermal diffusivity near $2 \times 10^{-6}\,\mathrm{m^2\,s^{-1}}$, but can increase to near $1 \times 10^{-3}\,\mathrm{m^2\,s^{-1}}$ at combustion temperatures. Most liquids are on the order of $1 \times 10^{-7}\,\mathrm{m^2\,s^{-1}}$ and solids are on the order of 1–2,000 $\times\, 10^{-7}\,\mathrm{m^2\,s^{-1}}$, with metallic solids around 2–5 $\times\, 10^{-5}\,\mathrm{m^2\,s^{-1}}$. Organic solids, including common explosives and their binders, generally fall into the range of 1–2 $\times\, 10^{-7}$.

Viscosity is the proportionality factor of Newton's law of viscosity, relating momentum flux (shear stress) to the velocity gradient. It appears in both the transient and steady state solution of the momentum equations, and also appears in Darcy's Law along with the permeability to relate flow to a pressure gradient. The simple kinetic theory can again be used to qualitatively understand the effect of the state variables on viscosity for gases:

$$\mu = \frac{2\sqrt{m\kappa T}}{3\pi^{3/2}d^2}. \tag{2.14}$$

As with thermal conductivity, there is no pressure dependence at normal conditions. Gas viscosities are on the order of 10^{-5} under normal conditions and can increase by a factor of 10 at combustion temperatures.

In the denser liquid phase, in order to translate, molecules must overcome an energy barrier presented by its neighbors. A kinetic theory approach therefore reveals an exponential dependence on temperature relative to the boiling temperature (T_b):

$$\mu = \frac{\rho N_\mathrm{a} h}{M} \exp\left[3.8\frac{T_\mathrm{b}}{T}\right], \tag{2.15}$$

where h is Planck's Constant. Examples of liquid viscosity are water: 1.75×10^{-3}; and engine oil: $3.85\,\mathrm{N\,s\,m^{-2}}$.

Kinematic viscosity is the ratio of the viscosity to density:

$$\nu = \frac{\mu}{\rho}. \tag{2.16}$$

Analogous to thermal diffusivity, this parameter may be thought of as the rate of diffusion of momentum. It always appears in the exponential terms of the transient solution of momentum problems; large values reflect short transients. An estimate of a system's time constant is given by

$$\tau \approx \frac{L^2}{\nu}. \tag{2.17}$$

Simple gases at STP have a kinematic viscosity near $1\text{–}25 \times 10^{-5}\,\mathrm{m^2\,s^{-1}}$ and the value does not change significantly near combustion temperatures. Liquids have a wide range of values; water at STP is 1.75×10^{-6}.

Mass diffusivity is the proportionality constant of Fick's law of diffusion and relates the flux of a molecular species to the concentration gradient. It appears in the solution to both the steady and unsteady solution of the species mass transport equations. Analogous to kinematic viscosity and thermal diffusivity, the dimensionless mass transfer Fourier number provides an estimate of the time constant of a system when its value is near unity:

$$\mathrm{Fo_{m,c}} = \frac{D\tau}{L^2} \approx 1. \tag{2.18}$$

Kinetic theory tells us that translational velocity increases with temperature, leading to a more rapid redistribution of species, and collision rates increase with increasing pressure, leading to a slower redistribution. The expression for a gas mixture consisting of nearly identical molecules (e.g., isotopes) shows the dependence on pressure and temperature:

$$D_{\mathrm{AA'}} = \frac{2}{3}\left(\frac{\kappa^3}{\pi^3 m}\right)\frac{T^{3/2}}{Pd^2}. \tag{2.19}$$

Diffusion gas phase coefficients for simple binary systems generally range from about 1 to $5 \times 10^{-5}\,\mathrm{m^2\,s^{-1}}$.

Similar to viscous momentum transport, diffusion in liquids is an "activated" process where molecules must overcome the barrier presented by nearby neighbors:

$$D \approx \kappa T\left(\frac{M}{\rho N_\mathrm{a} h}\right)^{2/3} \exp\left[-3.8\frac{T_\mathrm{b}}{T}\right]. \tag{2.20}$$

In practice, many factors influence the process. In most cases, empirical measurements are required and (2.20) can be used cautiously to extrapolate from known data. Typically, liquid diffusion coefficients are 10^5 times smaller than gases.

2.4 Transport Theory Equations

The equations governing transport processes have been developed *ad nauseum*, and there are many good texts covering each transport phenomenon. In particular, we suggest the text of Bird, Stewart, and Lightfoot as a comprehensive and detailed general text [46], and the aforementioned texts of Frank-Kamenetskii and Zeldovich for developments more specific to combustion and explosions. It is the intent of this text to provide a complete overview of nonshock initiation, and so we include a brief review of the formal development of transport theory.

The development of all three transport fields begins with the fundamental concept of the conservation laws: energy, mass, and momentum are conserved within a control volume. Within this very simple framework, and through the straightforward application of differential calculus, we can develop all of the transport equations.

It is always useful to begin with a very general form of the transport equations. Simplification is usually straightforward and a very general starting point allows us to see what assumptions must be made to arrive at the most tractable form for a particular situation. A balance on a differential volume equates energy stored and produced in the volume to the energy flux gradient:

$$-\nabla\phi = \frac{\partial h}{\partial t}, \tag{2.21}$$

where we have written storage and production in terms of enthalpy. For an Eulerian coordinate system (fixed reference frame) and in terms of temperature and heat capacity, we account for all fluxes (Fourier conduction and convection), storage and generation:

$$\rho c_p \left(\frac{\partial T}{\partial t} + (\mathbf{v} \cdot \nabla T) \right) = \nabla (k \nabla T) + \Delta h_{rxn} r (T, X) + \dot{q}, \tag{2.22}$$

where $\Delta h_{\text{rxn}} r (T, X)$ is the product of the enthalpy change associated with chemical reaction and the rate of that reaction. The rate, of course, generally depends exponentially on temperature and on some quantity related to the availability of reactants (X); for example, concentration of gas phase reactants or solid phase surface area (see Chap. 3.) $\dot{q}$ is the heat generated by any other source. In a Lagrangian reference frame (moving with the flow), we invoke the substantial derivative and we can simplify the equation to

$$\rho c_p \frac{DT}{Dt} = \nabla (k \nabla T) + \Delta h_{rxn} r (T, X) + \dot{q}. \tag{2.23}$$

The Lagrangian frame might be useful in the post-ignition regime when things begin to move or for the analysis of a propagating flame.

Specific enthalpy was used in this derivation. If we were to start the derivation with specific internal energy, the result would depend on the constant

volume heat capacity and reaction internal energy, rather than the constant pressure heat capacity and reaction enthalpy. The distinction is important as the former generally relates to incompressible media such as solids, liquids, and constant density gas phase processes. The latter generally applies to compressible gas phase processes. In this latter case, one must use caution with respect to reaction energy, as enthalpy is typically reported and the relationship between enthalpy and internal energy must be accounted for. Specifically,

$$\frac{\partial u}{\partial t} = \frac{\partial}{\partial t}\left(h - Pv\right) = \frac{\partial h}{\partial t} - v\frac{\partial P}{\partial t} - P\frac{\partial v}{\partial t}. \tag{2.24}$$

In general, all the material and thermodynamic properties can be space-, time-, and temperature-dependent.

There are three types of boundary conditions in heat transport analyses. These are the Dirlecht boundary conditions where we impose a surface temperature, T_s; the Neumann boundary conditions where we specify the heat flux, $\dot{q}_\mathrm{s}$, at the surface; and the Robin boundary conditions, which is a weighted hybrid of flux and temperature conditions. Mathematically, the Nuemann condition is

$$\mathbf{n} \cdot \left(-k\nabla T|_\mathrm{s}\right) = \dot{q}_\mathrm{s}. \tag{2.25}$$

The Robin boundary condition can take a general form that may account for convection normal (through) the boundary, convection parallel to the boundary, or conduction normal to the boundary:

$$\mathbf{n} \cdot \left(-k\nabla \mathbf{T}|_\mathrm{s} + \rho C_\mathrm{p}\mathbf{u}T_\mathrm{s}\right) = \mathbf{n} \cdot \left[\rho C_\mathrm{p}\mathbf{u}\left(T_\infty - T_\mathrm{s}\right] + h\left(T_\infty - T_\mathrm{s}\right).\right. \tag{2.26}$$

In these expressions, the subscript s indicates the boundary coordinate, ∞ indicates the condition far away from the system, and h is the heat transfer coefficient. The parameter h depends on the physical properties and movement (flow) of the medium surrounding the system. The method for computing h comes from boundary layer theory, and that discussion is beyond the scope of this text. However, simple methods to estimate h are readily available in the references provided [44, 46].

We arrive at the species transport equations by a similar route. Balancing the gradient of the mass flux ($\dot{n}_i$) with the mass density storage and production (r) of specie i in a differential volume leads to

$$-\nabla\dot{n}_i = \frac{\partial \rho_i}{\partial t} + r_i, \tag{2.27}$$

and we must account for each species present. Including convection transport, diffusion according to Fick's law and rewriting the equation in terms of the species mole fractions:

$$-\mathbf{v}\cdot\nabla\rho_i + \nabla\cdot\left(\rho_i D_{ij}\nabla x_i\right) = \frac{\partial \rho_i}{\partial t} + r_i\left(T, X\right), \tag{2.28}$$

where x_i is the mole fraction of species i. This is a very general (and difficult to apply) form of the species mass transport equation with no restriction on

constant density or diffusion coefficient. However, this form is only valid for binary systems, and in general the derivation of equations for more than two components with nonconstant density is difficult. If we make the assumption of constant density and diffusion coefficient, the more familiar diffusion equation results (Eulerian coordinates):

$$\frac{\partial C_i}{\partial t} + \mathbf{v} \cdot \nabla C_i = D_{i,n} \nabla^2 C_i + r_i\,(T, X), \tag{2.29}$$

and in Lagrangian coordinates,

$$\frac{DC_i}{Dt} = D_{i,n} \nabla^2 C_i + r_i\,(T, X). \tag{2.30}$$

These forms are most valid for dilute solutions at constant temperature and pressure. Of course, those conditions do not describe most of the interesting explosives problems, but there is insight to be gained by the application of simplified theory. Most notably, researchers have applied (2.29) with its heat transport analog (2.22) to describe flame structure [19]. The codependency of these equations of course arises through the heat and species generation term, which depend on temperature and the quantity X that relates to concentration. Two notable assumptions exist to decouple the equations. If the Lewis number,

$$Le = \frac{\rho C D}{k}, \tag{2.31}$$

is close to unity, the concentration and temperature fields are similar. And the assumption of zero-order chemical reaction allows decoupled solution of the heat and species transport equations. The boundary conditions for the species transport equations are analogous to those for heat transport. We can specify a Dirlecht condition at the boundary (concentration), a Nuemann condition (species flux), or the Robin hybrid condition.

The velocity fields of (2.22) and (2.29), if they exist, are computed using the principle of conservation of momentum. As with heat and species transport, momentum transport occurs by convection and by molecular collisions (i.e., conduction or diffusion.) While these two mechanisms cause transport in parallel for heat and species transport, convective momentum transport by fluid motion is orthogonal to transport by molecular collisions. Consequently, the derivation leads to second order tensor expressions. The full derivation of the governing equation falls into the fluid mechanics field of study. Formal application of the full equation is rare in our field of study, but for completeness we provide what is commonly referred to as the Navier–Stokes equation:

$$\mu \nabla^2 \mathbf{v} - \nabla P = \rho \left(\frac{\partial \mathbf{v}}{\partial t} + \mathbf{v} \cdot \nabla \mathbf{v} \right), \tag{2.32}$$

where this form requires a constant density and viscosity (μ). Note that the product of the gradient operator vector and the velocity vector and the

Laplacian operator vector and the velocity vector are both dyadic products and the result is a tensor.

The application of the Navier–Stokes equation to nonshock initiation problems requires a level of computing power not generally available. In lieu of those equations, researchers have applied Darcy's law of permeation in porous media as an approximation for creeping flow conditions (low Reynold's number, $Re < 10$):

$$\mathbf{v}_\mathrm{s} = \frac{-\kappa}{\mu}\nabla P, \tag{2.33}$$

where κ is the permeability and $\mathbf{v}_\mathrm{s}$ is the superficial velocity vector. In the preignition regime, the movement of chemical species under the influence of a pressure gradient has only recently been incorporated into analysis [5], and we will review that work in a later section. Of course, conditions in the post-ignition regime do not meet the creeping flow requirement and we must apply the Navier–Stokes equations along with the science of Multi-phase Computational Fluid Dynamics to provide meaningful solutions.

We see the further interplay of transport processes that occurs through the pressure gradient term in both the Darcy approximation and the Navier–Stokes equation. The pressure gradient must be found from the production of chemical species via coupling with the heat and species transport equations. Strictly speaking, we must simultaneously consider all three transport phenomena and the interplay originates both from chemical reaction heat and species generation and the thermodynamic linkage of pressure, temperature and density. Consideration of fully coupled transport theory remains a significant challenge, mainly due to limitations of computing (and funding) resources.

2.5 Selected Examples of Transport Theory Applied to Explosive Problems

We will review three recent cases where transport theory has been applied to problems involving explosives. First, to more fully understand the fundamentals of hot spot initiation, we have chosen a model system for study that uses the internal and localized dissipation of microwave energy to generate hot spots [47]. Next we will review a boundary-heated problem that includes species and momentum transport. Zerkle has invoked Darcy's Law for a boundary-heated problem and he showed that permeation of decomposition products through the bulk of the explosive was required to more accurately predict temperature profiles and the violence of reaction [5]. Finally, we discuss a post-ignition problem having coupled heat and species transport. The work of Ward et al. used a low activation energy kinetic expression to characterize the combustion of HMX and made assumptions about the similarity between the thermal and species diffusion coefficients [7].

Theory of microwave-induced hot spots. Organic explosives generally interact weakly with electromagnetic energy in the microwave frequency range. Therefore, the addition of electromagnetically absorbing inclusions provides a tractable system for the study of localized heating and ignition phenomena. The work considered the connections amongst the theories of dielectric mixing, microwave absorption, heat transfer, and thermal ignition theory in order to understand a model system of idealized hot spots; namely, small high thermal conductivity spherical inclusions (<100 μm) dispersed within a homogeneous low thermal conductivity explosive. The advantage to this mode of heating compared to "normal" hot spot mechanisms is that electromagnetic excitation isolates purely thermal effects while the others rely upon mechanical stimulation of material. Here, we review the work of Perry and Glover [47], and use dimensionless numbers to illuminate dominant mechanisms and to simplify the problem [44, 46].

The most generic solution to this problem is found by writing (2.22) for both the region inside the inclusion ($0 < r < R$) and the region outside the inclusion ($R < r < \infty$). For the region inside the inclusion, we use the microwave heat generation term

$$\dot{q} = \omega \varepsilon_i'' \frac{E^2}{2}, \tag{2.34}$$

where ω is the microwave angular frequency, ε_i'' is the dielectric loss (absorptivity) of the inclusion, and E is the electric field strength near the inclusion. For the region outside the inclusion, we use a zero-order form of the Arrhenius reaction term. The problem is solved by using a flux-matching boundary condition at the interface ($r = R$), a symmetry boundary condition at $r = 0$, and the initial temperature far away from the inclusion ($r = \infty$). Finding the time and spatially dependent temperature behavior requires a numerical solution of the coupled set of equations for $r < R$ and $r > R$.

However, in the case of microwave hot spot generation, the heat transport properties of a typical high thermal conductivity microwave absorbing inclusion (e.g., silicon carbide) suggest that the low thermal conductivity explosive surrounding the hot spot will limit the rate of heat transport. This is shown formally by evaluating the dimensionless Biot number:

$$Bi = \frac{2hR}{k_{\mathrm{i}}}, \tag{2.35}$$

where h is the heat transfer coefficient and the subscript i refers to the inclusion. The heat transfer coefficient is found using the dimensionless Nusselt number:

$$Nu = \frac{2hR}{k_{\mathrm{e}}}, \tag{2.36}$$

where the subscript e refers to the explosive. For a sphere in a stationary medium, the Nusselt number is exactly 2 and

$$h = \frac{k_{\mathrm{e}}}{R}. \tag{2.37}$$

For $k_e \ll k_i$ and small R, $Bi \ll 1$ and the transport equation for $R < r < \infty$ will adequately describe the behavior. Equation (2.22) in spherical coordinates for the region outside the inclusion is

$$[\rho c_p]_e \frac{\partial T}{\partial t} = k_e \frac{1}{r^2} \frac{\partial}{\partial r}\left(r^2 \frac{\partial T}{\partial r}\right) + \frac{\rho_e \Delta h_{rxn}}{M} r(T, X). \tag{2.38}$$

Let

$$\theta = \frac{T - T_\infty}{T_{ig} - T_\infty}; \;\; \xi = \frac{r}{R}, \tag{2.39}$$

and we use a Fourier number to define a dimensionless time

$$\tau = \frac{\alpha_e t}{R^2}. \tag{2.40}$$

The dimensionless form of the equations is then

$$\frac{\partial \theta_e}{\partial \tau} = \frac{1}{\xi^2} \frac{\partial}{\partial \xi}\left(\xi^2 \frac{\partial \theta_e}{\partial \xi}\right) + \left\{ \frac{\rho \Delta h_{rxn} R^2}{M k_e \left(T_{ig} - T_\infty\right)} A \exp\left[- \frac{E_a}{R\left(\theta_e \left(T_{ig} - T_\infty\right) + T_\infty\right)} \right] \right\}, \tag{2.41}$$

where the expression in brackets is the dimensionless Damköhler number, relating the rate of heat conduction to the rate of heat production by chemical reaction. The boundary condition is

$$\frac{\dot{q} R^2}{3 k_e (T_{ig} - T_\infty)} = \frac{\omega \varepsilon_i'' E^2 R^2}{6 k_e \left(T_{ig} - T_\infty\right)} = - \left. \frac{\mathrm{d}\theta}{\mathrm{d}\xi} \right|_{\xi = 1} = \dot{\Theta}. \tag{2.42}$$

Because of microwave skin depth effects, R must be less than $\sim$100 μm. Even with this abbreviated statement of the problem, a numerical solution is required to find the evolution of the temperature profiles around the hot spot and the time to ignition. However, we can learn salient features about the behavior of the system without the full solution. From our general understanding of hot spot ignition, we know the following physical criteria must be met for ignition to occur:

1. Microwave energy dissipation must exceed heat removal at the ignition temperature.
2. The rate of heat production via exothermic chemistry must exceed the rate of heat transport away from the inclusion at the ignition temperature.

Equation (2.42) provides the relationship for condition 1. The dimensionless gradient at the inclusion surface must exceed unity for the hot spot to reach the ignition temperature. To find the ignition temperature, we use the Damköhler number in (2.41) to find when condition 2 is true and use that information to determine the ignition temperature. By definition, $\theta = 1$ when reaction heat exceeds heat removal by conduction:

$$\frac{\rho \Delta h_{rxn} R^2}{M k_e (T_{ig} - T_\infty)} A \exp\left[- \frac{E_a}{R T_{ig}} \right] = 1. \tag{2.43}$$

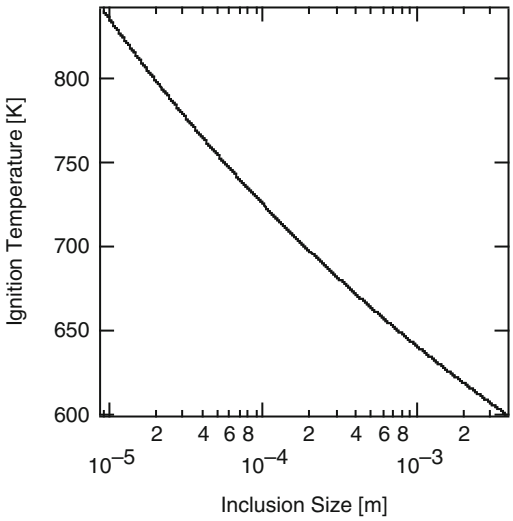

Fig. 2.1. The relationship between ignition temperature and hot spot inclusion size for HMX

This transcendental equation must be solved iteratively to find T_{ig}. Figure 2.1 shows the relationship of T_{ig} and hot spot size for values representative of the kinetic, thermochemical, and thermophysical parameters of HMX.

We have learned two very important features of this system without solving the governing equations: the ignition temperature and the minimum microwave power dissipation required to reach the ignition temperature. However, we cannot deduce the heating rate or the time required to reach the ignition temperature from this approach. If we do not care about the exact nature of the spatial temperature profiles, we can further simplify the problem by ignoring the spatial dependence and performing an energy balance on the inclusion. The balance leads to a dimensionless equation describing the temperature of the inclusion (recall $Nu = 2$ for a stagnant medium):

$$\frac{\mathrm{d}\theta}{\mathrm{d}\tau'} = 3(\dot{\Theta} - \theta) \tag{2.44}$$

where

$$\tau' = \frac{k_{\mathrm{e}}}{\rho_{\mathrm{i}} C_{\mathrm{i}}} \frac{t}{R^2} \tag{2.45}$$

and the solution is

$$\theta = \dot{\Theta}\left[1 - \exp\left(-3\tau'\right)\right]. \tag{2.46}$$

The dimensionless time to ignition is

$$\tau'_{\mathrm{ig}} = -\frac{1}{3} \ln\left(1 - \frac{1}{\dot{\Theta}}\right). \tag{2.47}$$

This straightforward development illuminates the temporal qualities of the system. Mathematically, ignition will never occur for $\dot{\Theta} < 1$, a condition identical to the statement derived from the dimensionless boundary condition of (2.42). Here, we have used R for the characteristic dimension. This most accurately (but still qualitatively) shows the transient behavior prior to ignition for larger values of $\dot{\Theta}$; that is, $\dot{\Theta} > 5$. For values of $\dot{\Theta}$ closer to unity, a characteristic length between R and $2R$ is more accurate.

The dielectric loss (ε_i'' of (2.34)) of the inclusion depends on its electrical conductivity and the permittivity of the explosive medium. Generally, inclusions embedded in a low permittivity medium that are less than 100 μm in size and that have a conductivity in the semiconductor range (10 ohm) have a high dielectric loss $\left(\sim 70 \times 10^{-12}\ \mathrm{F\,m^{-1}}\right)$, leading to a high rate of energy dissipation [47]. High frequency also favors a high dissipation rate (2.34). Figure 2.2 shows the transient inclusion temperature and Fig. 2.3 shows the dimensionless ignition time over a range of dimensionless microwave power dissipation values ($\dot{\Theta}$). While this analysis was qualitative, it illuminates the factors important to microwave hot spot ignition. More importantly, we may apply the analysis for any heating stimulus as long as we can satisfy the stated assumptions and find an appropriate expression for $\dot{\Theta}$.

Boundary heating problem including species and momentum transport. In the early 2000s, researchers at Los Alamos conducted a series of large-scale (10 kg) PBX 9501 cookoff experiments (the Large Scale Annular Cookoff experiment: LSAC.) The annular charges (8.9 cm i.d., 15.9 cm o.d.) were held at a temperature sufficient to drive sublimation and decomposition reactions (∼180°C) and the $\beta - \delta$ phase transition such that substantial thermal

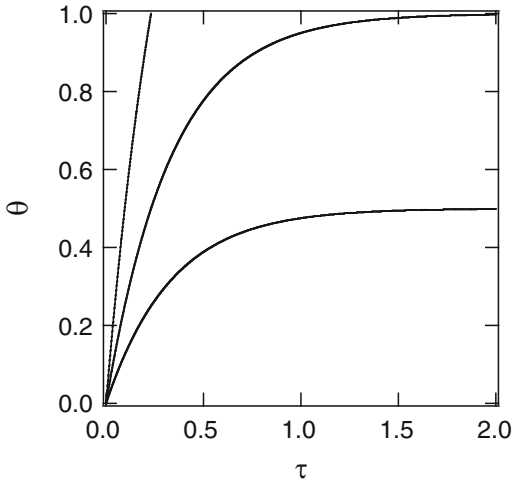

Fig. 2.2. The dimensionless transient inclusion temperature for three values of the dimensionless microwave heating term: 0.5, 1, and 5

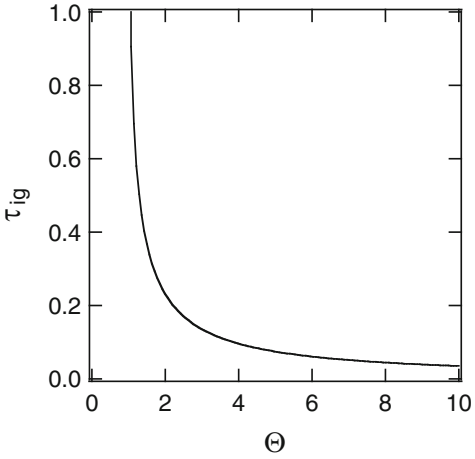

Fig. 2.3. Dimensionless ignition time as a function of dimensionless microwave power dissipation. There is a threshold below which ignition will not occur

damage occurred; that is, significant porosity developed. These experiments were highly instrumented for the primary purpose of calibrating cookoff models that attempt to predict the explosion violence after ignition. The boundary conditions that lead to ignition have already been well established and documented in modern texts [48]. However, ignition theory does not tell us anything about the post-ignition explosive behavior. It was suspected, a priori, that the high degree of porosity generated during the heating phase would facilitate movement of reactive decomposition products through the charge and potentially affect both the pre- and post-ignition behavior. Indeed, it was found that the models could not accurately predict temperature profiles without including the movement of reactive species by momentum transport. Both the temperature field and distribution of reactive species affect the post ignition behavior, making the incorporation of species and momentum transport an important step towards understanding explosion violence. As modeling of the LSAC is an excellent example of the application of heat transport theory coupled with species and momentum transport, we will review the work of David Zerkle towards this end [5].

The model development began by writing the species transport equation (e.g., (2.28)) for a multiphase system:

$$\frac{\partial\left(\phi_i \rho_i\right)}{\partial t} + \nabla \cdot \left(\phi_i \rho_i \mathbf{v}_{\mathrm{g}}\right) = r\left(T, X\right), \tag{2.48}$$

where ϕ_i is the species volume fraction. Compressible gas phase processes were important to this analysis, and the heat transport equation was derived in terms of internal energy. The convective transport term of (2.22) was written as

$$\nabla \cdot \left[\phi_{\mathrm{g}} \rho_{\mathrm{g}} \mathbf{v}_{\mathrm{g}} \left(u_{\mathrm{g}} + \frac{P_{\mathrm{g}}}{\rho_{\mathrm{g}}} \right) \right], \tag{2.49}$$

where the subscript g refers to the gas phase. The specific internal energy is related to temperature through (2.4); pressure and temperature are related by the ideal gas equation of state. These relations lead to the following form of the heat transport equation:

$$\rho C_{\mathrm{v}} \frac{\partial T}{\partial t} + \nabla \cdot \left(\phi_{\mathrm{g}} \rho_{\mathrm{g}} \mathbf{v}_{\mathrm{g}} C_{\mathrm{pg}} T \right) = \nabla \left(-k \nabla T \right) + \Delta u_{\mathrm{rxn}} r \left(T, X \right). \tag{2.50}$$

In lieu of incorporating the multiphase momentum transport equations, the velocity field was found using Darcy's law (2.33) where $\mathbf{v}_{\mathrm{s}} = \phi_{\mathrm{g}} \mathbf{v}_{\mathrm{g}}$. The permeability for a range of thermal damage conditions was determined from the small-scale experiments of Parker et al. [49]. The overall effective density, heat capacity, and thermal conductivity were computed from (respectively):

$$\rho = \sum\nolimits_i \phi_i \rho_i; C_{\mathrm{v}} = \frac{\sum_i \phi_i \rho_i C_v}{\rho}; \text{ and } k = \sum\nolimits_i \phi_i k_i. \tag{2.51}$$

The reaction term (r) was modeled using the Los Alamos four-step decomposition mechanism that includes the endothermic solid phase transition, the endothermic sublimation of HMX, and the exothermic gas phase reactions [50]. The coupling of momentum, species, and heat transport in this system comes about through the thermodynamic state of the system, where, in this case, the ideal gas law equation of state ties pressure, temperature, and density together and the system is driven by the reactive production (or consumption) of heat and species.

The partial differential equation solver, Flex PDE [51], provided the temperature, species concentration, and velocity fields. Figure 2.4 shows the computed temperature profiles, which agree well with the experimentally measured values. Figure 2.5 shows the comparison of temperature profiles with and without including flow, just prior to ignition. The inclusion of flow indicated a much larger volume at a higher temperature and that reactive species were also spread through a large portion of the charge. These two factors mean that the material was primed for faster reaction spreading, hence more violent explosion. Finally, the reader might notice the asymmetry in the results. This comes about from variations in contact resistance imposed on the interface between the explosive and its container. This experiment is discussed more fully in Chap. 7.

A laminar flame model. We have examined two preignition scenarios, and now we examine the post-ignition transport phenomena associated with laminar burning of HMX. While we are most interested in violent explosion, the physical processes that occur for laminar burning also occur during violent explosion. Most explosive combustion processes are surface phenomena: combustible gases evolve from a solid surface and burn in the gas phase at a well defined "stand-off" from that surface. Pressure controls the stand-off distance.

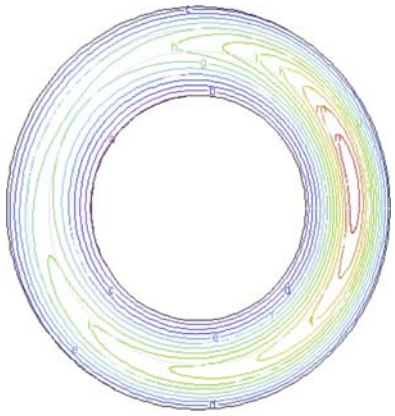

Fig. 2.4. Calculated temperature profiles just prior to ignition for the annular cookoff shot. The calculation included Darcy flow and agreed well with experimental measurements. The boundaries were held at 180°C and the highest temperature contour was 220°C. The contour intervals are approximately 2.86°C. The inner diameter was 8.9 cm and the outer diameter was 15.9 cm

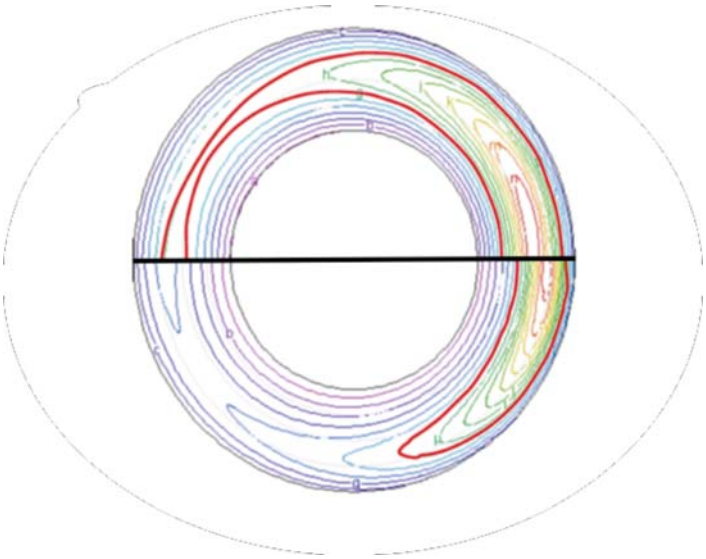

Fig. 2.5. Comparison between temperatures computed with (*upper*) and without (*lower*) species and momentum (Darcy) transport just prior to ignition. The highest temperature contours are 220°C. The lowest temperature contour with Darcy flow was 198°C and the lowest temperature contour without flow was 191°C

The essential difference between laminar burning and violent explosion is that laminar burning occurs over a surface area much larger than any defects, pores, cracks, grains, etc. in that surface and the stand-off is also much larger than

those surface features. Violent explosive burning occurs when the pressure squeezes the flame stand-off to a dimension on the order of the aforementioned feature sizes, forcing hot combustion products into the cracks and pores, such that combustion occurs on a high surface area within the bulk of the material. Convective (momentum transport driven) processes of course play the dominant role in this regime, but the fundamental process of surface gas evolution and burning near the surface that occur during laminar combustion still occur in the violent explosion regime. Because of the relevance of the laminar analysis to the whole range of ignition response, we will review the work of Ward and Son [7]. Those authors develop the heat and species transport equations for the laminar flame and provide a straightforward and illuminating analytical solution that correctly describes experimentally observed flame structure of burning HMX, which is shown in Fig. 2.6.

Their analysis consisted of two parts: development of the steady-state heat transport equation with a high activation energy decomposition reaction for the solid phase and the steady-state coupled heat and mass transport equations with very low activation energy exothermic combustion reactions for the gas phase. One-dimensional cartesian coordinates were used with the origin at the solid–gas interface for both regions.

For the solid phase, (2.22) was reduced to

$$\widetilde{m}c_{\mathrm{p}}\frac{\partial T}{\partial x} = k_{\mathrm{e}}\frac{\partial^2 T}{\partial x^2} + \Delta h_{\mathrm{d}} r\,(T), \tag{2.52}$$

where the subscript d refers to the decomposition reaction

$$\mathrm{HMX} \rightarrow I, \tag{2.53}$$

where I is a representative gas phase intermediate. The kinetic expression is

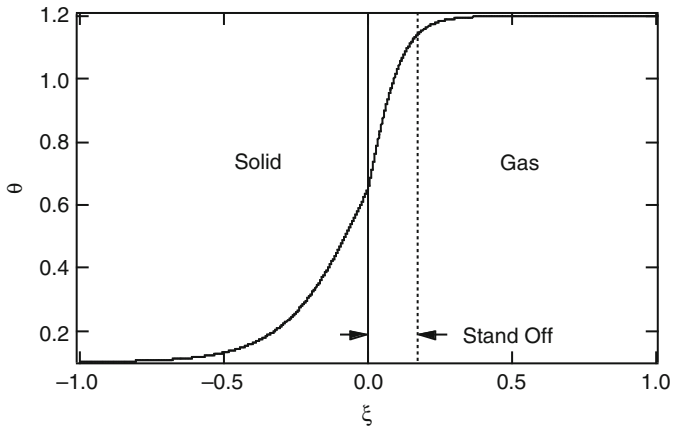

Fig. 2.6. The quantitative laminar flame temperature structure predicted by Ward et al.

$$r\left(T\right) = \rho_{\mathrm{e}} A_{\mathrm{d}} \exp\left(-\frac{E_{\mathrm{d}}}{RT}\right). \tag{2.54}$$

The symbol $\tilde{m}$ is the mass flux and was the variable in the final solution that represented the "feed" of gas phase reactants for the gas phase part of the analysis. It is also the parameter that translates into a burning rate and is thus a parameter of primary interest. A floating boundary Dirlecht boundary condition, T_{s}, was specified at the solid–gas interface and ambient temperature in the solid bulk ($T = T_0$ @ $x = -\infty$) provided the second boundary condition. Merzhanov and Dubovitskii [52] provided the original solution for the mass flux:

$$\widetilde{m}^2 = \frac{A_{\mathrm{d}} R T_{\mathrm{s}}^2 k_{\mathrm{e}} p_{\mathrm{e}} \cdot \exp\left(-E_{\mathrm{d}}/RT_{\mathrm{s}}\right)}{E_{\mathrm{d}}\left[c_{\mathrm{p}}\left(T_{\mathrm{s}} - T_0\right) - \Delta h_{\mathrm{d}}/2\right]}. \tag{2.55}$$

To develop the problem in the gas phase, the authors began with the assumption of equality between the molar heat capacity of the gas and solid phase, and that the dimensionless Lewis number was unity:

$$Le \equiv \frac{\alpha_{\mathrm{g}}}{D} = 1, \tag{2.56}$$

where the subscript g refers to the gas phase. These assumptions are reasonably accurate and they substantially simplify the problem. Expressing the governing equations in terms of dimensionless variables further facilitates the solution; the following relationships were used:

$$\begin{aligned} &\theta = \frac{T}{T_\infty - T_{-\infty}};\ \ E^* = \frac{E}{R\left(T_\infty - T_{-\infty}\right)};\ \ \Delta h_i^* = \frac{\Delta h_i}{C_{\mathrm{p}}\left(T_\infty - T_{-\infty}\right)};\\ &\xi = \frac{x\tilde{m}_{\mathrm{r}} c_{\mathrm{p}}}{k_{\mathrm{g}}};\ \ \text{and}\ \ \tilde{m}^* = \frac{\tilde{m}}{\tilde{m}_{\mathrm{r}}}, \end{aligned} \tag{2.57}$$

where $\tilde{m}_{\mathrm{r}}$ is a reference mass flux. These definitions lead to the following dimensionless and steady forms of (2.22) (heat) and (2.29) (species):

$$\widetilde{m}^* \frac{\partial \theta}{d\xi} = \frac{\partial^2 \theta}{\partial \xi^2} - Da_{\mathrm{h}} \ \text{ and } \ \widetilde{m}^* \frac{\partial X}{d\xi} = \frac{\partial^2 X}{\partial \xi^2} + Da_{\mathrm{s}}, \tag{2.58}$$

where X is the mass fraction of I and Da_{h} and Da_{s} are the heat (h) and species (s) transport Damköhler numbers. The boundary conditions were

$$\theta\left(0\right) = \theta_{\mathrm{s}};\ \ \theta\left(\xi \to \infty\right) = \theta_{\mathrm{f}};\ \ X\left(0\right) = X_{\mathrm{s}};\quad \text{and}\quad X\left(\xi \to \infty\right) = 0. \tag{2.59}$$

The similarity of the two equations and the fact that $Le = 1$ leads to a relationship between the mass fraction and the dimensionless temperature:

$$X = \frac{\theta_{\mathrm{f}} - \theta}{\Delta h_{\mathrm{c}}^*}, \tag{2.60}$$

where the subscript c refers to the gas-phase combustion reaction. The route leading to this relationship is not entirely straightforward, and we refer the

reader to Zeldovich for the derivation [53]. The gas phase reaction was assumed to be of the form

$$I + X \rightarrow C + X, \tag{2.61}$$

and the kinetic expression was

$$r\left(T, X\right) = \left(\frac{PM}{R}\right)^2 A_{\mathrm{c}} \exp\left(-\frac{E_{\mathrm{c}}}{RT}\right) X. \tag{2.62}$$

Using (2.60), the Damköhler numbers are

$$Da_{\mathrm{h}} = Da^* \left(\theta_f - \theta\right) \exp\left(-\frac{E_{\mathrm{c}}^*}{\theta}\right);\ Da_{\mathrm{s}} = Da^* X \exp\left(-\frac{E_{\mathrm{c}}^*}{\theta_{\mathrm{f}} - X\Delta h_{\mathrm{c}}^*}\right), \tag{2.63}$$

where

$$Da^* = \frac{k_{\mathrm{g}} A_{\mathrm{c}}}{c_{\mathrm{p}}} \left(\frac{P \cdot M}{\tilde{m}_{\mathrm{r}} R}\right)^2. \tag{2.64}$$

They still required a numerical solution for a nonzero E^*; however, an essential feature of this work was the authors' recognition that a solution using high gas phase activation energy did not qualitatively predict experimentally observed temperatures and they investigated the solution behavior using a very small gas phase activation energy. In the limit, $E_{\mathrm{c}}^* \rightarrow 0$ had the added benefit of allowing an analytical solution. In dimensionless variables the temperature and concentration profiles were

$$\frac{X}{X_{\mathrm{s}}} = \frac{\theta - \theta_f}{\theta_{\mathrm{s}} - \theta_f} \exp\left(\frac{\xi}{\xi_{\mathrm{g}}}\right), \tag{2.65}$$

where ξ_{g} the dimensionless flame stand-off distance is

$$\xi_{\mathrm{g}} = \frac{2}{\sqrt{\tilde{m}^{*2} + 4Da^*} - \tilde{m}^*}. \tag{2.66}$$

The dimensionless form of the mass flux expression (2.55) is

$$\tilde{m}^{*2} = \frac{A_{\mathrm{d}} \theta_{\mathrm{s}}^2 \exp\left(-E_{\mathrm{d}}/\theta_{\mathrm{s}}\right)}{E_{\mathrm{d}} \left[\theta_{\mathrm{s}} - \theta_{-\infty} - \Delta h_{\mathrm{d}}^*/2\right]}, \tag{2.67}$$

and the surface temperature was

$$\theta_{\mathrm{s}} = \theta_{-\infty} + \Delta h_{\mathrm{d}}^* + \frac{\Delta h_{\mathrm{c}}^*}{\xi_{\mathrm{g}} \tilde{m}^* + 1}. \tag{2.68}$$

The '$-\infty$' subscript in these equations refers to the far upstream (initial) condition. Unfortunately, after systematically following the route of non-dimensionalization, the Lewis number assumption, determination of the surface temperature and mass flux required iteration. What the authors found, however, is that the low activation energy assumption indeed resulted in a

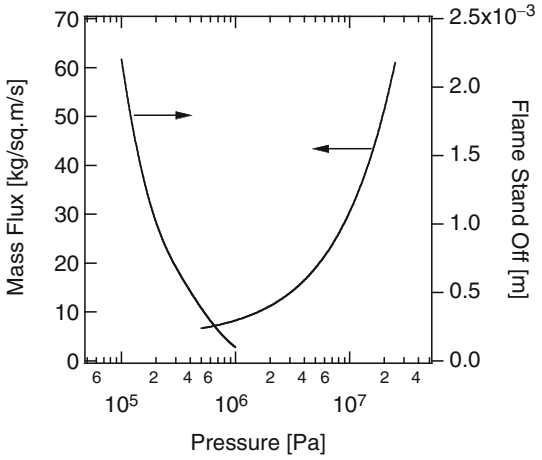

Fig. 2.7. Mass flux from solid to gas and the flame stand-off distance as a function of pressure according to Ward et al.

fairly accurate prediction of temperature profiles, mass flux, stand-off, and surface temperature. Furthermore, the theory correctly predicts the effect of pressure:

$$\tilde{m} \propto P^n, \tag{2.69}$$

where $n \approx 0.85$, as shown in Fig. 2.7, was also in good agreement with experimental observations. We have known for some time that the burning rate of solid propellants follows this type of pressure relationship, often referred to as Vielle's law. This relationship, however, was empirically determined, whereas the relationships leading to the theoretically determined behavior depend on physical parameters and thereby provide insight to the factors that affect the overall behavior. The theory also reveals how flame stand-off depends on pressure and this is also shown in Fig. 2.7. This behavior is particularly important; as mentioned above, the flame stand-off distance relative to characteristic surface defect dimensions determines the pressure at which laminar deflagration transits to violent explosion.

2.6 Summary

In this chapter, we have discussed the general framework of transport phenomena and their central role as the theory that describes ignition and combustion behavior. The development of this theory has a rich and interesting history. Undoubtedly, in all fields of study, creative and insightful individuals advance the state of the art, and our field is no exception. We have measured or we can compute (or estimate, to a reasonable degree) the physical properties of transport theory, we know the conservation-based equations of

transport theory, and we can therefore compute solutions to many important problems. However, in the modern era of advanced numerical solutions, we must remain cognizant of the important physical processes that govern ignition and combustion behavior. Progress requires computational advancement while maintaining our intuitive understanding.

References

1. Tarver, C.M., Tran, T.D.: Thermal decomposition models for HMX-based plastic bonded explosives. Combust. Flame **137**, 50–62 (2004)
2. Kubota, N.: Survey of rocket propellants and their combustion characteristics. In: Kuo, K.K., Summerfield, M. (eds.) Fundamentals of Solid-Propellant Combustion, Progress in Astronautics and Aeronautics, vol. 90. American Institute of Aeronautics and Astronautics, New York (1984)
3. Prasad, K., Yetter, R.A., Smooke, M.D.: An eigenvalue method for computing the burning rates of HMX propellants. Combust. Flame **115**, 406 (1998)
4. Perry, W.L., Dickson, P.M., Parker, G.R., Smilowitz, L.B., Henson, B.F., Asay, B.W.: Factors affecting explosive reaction violence in PBX 9501. In: Proceedings of the 13th International Detonation Symposium (2006)
5. Zerkle, D.K., Luck, L.B.: Modeling cook-off of PBX 9501 with porous flow and contact resistance, Los Alamos National Laboratory document LA-UR-03-8077; or 21st JANNAF Propulsion Systems Hazards Subcommittee Proceedings CD# JSC-CD-24 (2003)
6. Zeldovich, Y.: Flame propagation in a substance reacting at initial temperature. Combust. Flame **39**, 219–224 (1980)
7. Ward, M.J., Son, S.F., Brewster, M.Q.: Steady deflagration of HMX with simple kinetics: A gas phase chain reaction model. Combust. Flame **114**, 556–568 (1998)
8. Kumar, M., Kuo, K.K.: Flame spreading and ignition transients. In: Kuo, K.K., Summerfield, M. (eds.) Fundamentals of Solid-Propellant Combustion, Progress in Astronautics and Aeronautics, vol. 90. American Institute of Aeronautics and Astronautics, New York **305** (1984)
9. Asay, B.W., Son, S.F., Bdzil, J.B.: The role of gas permeation in convective burning. Int. J. Multiphas. Flow **22**(5), 923–952 (1996)
10. Parker, G.R., Peterson, P.D., Asay, B.W., Dickson, P.M., Perry, W.L., Henson, B.F., Smilowitz, L.B., Oldenborg, M.R.: Examination of morphological changes that affect gas permeation through thermally damaged explosives. Propellants, Explosives and Pyrotechnics **29**, 274 (2004)
11. Zerkle, D.K., Asay, B.W., Parker, G.R., Dickson, P.M., Smilowitz, L.B., Henson, B.F.: On the permeability of thermally damaged PBX 9501. Propellants, Explosives and Pyrotechnics **32**, 251 (2007)
12. Baer, M.R., Nunziato, J.W.: A two-phase mixture theory for the deflagration-to-detonation transition (DDT) in reactive granular materials. Int. J. Multiphas. Flow **12**(6), 861–889 (1986)
13. McAfee, J.M., Asay, B.W., Bdzil, J.B.: Deflagration-to-detonation in granular HMX: ignition, kinetics and shock formation. In: Proceedings of the 10th International Detonation Symposium, 716 (1993)

14. Faraday, M.: The Chemical History of a Candle. Cherokee Publishing Company, Atlanta, Georgia (1993)
15. Mallard, E.F.: Ann. Mine. 7, 355 (1875)
16. Mallard, E.F., Le Chatelier, H.: Combustion of explosive gas mixtures. Ann. Mine. (1883)
17. van't Hoff, J.H.: Lectures on Theoretical and Physical Chemistry, Lehfeld, R.A. (trans.). Arnold, London (1899)
18. Zeldovich, Y.B.: On the theory of flame propagation. Zh. Fiz. Khim. **22**, 27 (1928)
19. Zeldovich, Y.B., Barenblatt, G.I., Librovich, V.B., Makhviladze, G.M.: The Mathematical Theory of Combustion and Explosions (English Translation). Consultants Bureau, New York (1985); Original Russian text: Nauka Press, Moscow (1980)
20. Belyaev, A.F.: Zh. Fiz. Khim. **12**, 93 (1938)
21. Todes, O.M.: Zh. Fiz. Khim. **4**, 78 (1933)
22. Seminov, N.N.: Z. Phys. Chem. **48**, 571.(1928)
23. Frank-Kamenetskii, D.A.: Zh. Fiz. Khim. **13**, 738 (1939)
24. Frank-Kamenetskii, D.A.: Diffusion and Heat Transfer in Chemical Kinetics, Appleton, J.P. (trans.). Plenum Press, New York (1969); Original Russian text: Nauka Press, Moscow (1947)
25. Bowden, F.P., Stone, M.A., Tudor, G.K.: Proc. Roy. Soc. Lond. A **188**, 329 (1947)
26. Rideal, E.K., Robertson, A.J.B.: Proc. Roy. Soc. Lond. A **195**, 135 (1948)
27. Merzhavanov, A.G., Barzykin, V.V., Gontkovskaya, V.T.: A problem of local thermal explosion. Dolk. Akad. Nauk SSSR **148**(2), 380 (1963)
28. Field, J.E., Bourne, N.K., Palmer, S.J.P., Wallery, S.M.: Hot-spot ignition mechanisms for explosives and propellants. In: Field, J.E., Grey, P. (eds.) Energetic Materials. The London Royal Society, London (1992)
29. Eirich, F.R., Tabor, D.: Proc. Camb. Phil. Soc. **44**, 566 (1948)
30. Bowden, F., Yoffe, A.: Initiation and Growth of Explosion in Liquids and Solids. Cambridge Monographs on Physics, Cambridge University Press, Cambridge (1952)
31. Afanas'ev, G.T., Bobolev, V.K.: Initiation of Solid Explosives by Impact, Jerusalem Israel Program for Scientific Translations (1971)
32. Langevin, A., Bicquard, P.: Memor. Proud. **26**, 354 (1934)
33. Wyatt, R.M., Moore, P.W., Adams, G.K., Summer, J.F.: Proc. Roy. Soc. Lond. A **246**, 189 (1958)
34. Tucker, T.J.: Spark initiation requirements of a secondary explosive. Ann. New York Acad. Sci. **152**, 643–653 (1968)
35. Griffith, N., Groocock, J.M.: The burning to detonation of solid explosives. J. Chem. Soc. Lond. **814**, 4154–4162 (1960)
36. Andreev, K.K., Belyaev, A.F.: The Theory of Explosives. Oborongiz, Moscow (1960)
37. Taylor, J.W.: The burning of secondary explosive powders by a convective mechanism. Trans. Faraday Soc. **58**, 561 (1962)
38. Kuo, K.K., Summerfield, M. (eds.): Fundamentals of Solid-Propellant Combustion. American Institute of Aeronautics and Astronautics, New York (1984)
39. Bernecker, R.R., Price, D.: Studies in the transition from deflagration to detonation in granular explosives III. Combust. Flame **22**, 161–170 (1974)

40. Gibbs, T.R., Popalato, A.: LASL Explosive Property Data. University of California Press, CA (1981)
41. Dobratz, B.M., Crawford, P.C.: LLNL Explosives Handbook. National Technical Information Service, US Department of Commerce, Springfield, VA (1985)
42. Lee, D.R.: CRC Handbook of Chemistry and Physics, 88th edn. CRC Press, FL (2007)
43. NIST Chemistry WebBook, http://webbook.nist.gov/chemistry/
44. Incropera, F.P., Dewitt, D.P.: Fundamentals of Heat and Mass Transfer, 5th edn. Wiley, New York (2002)
45. Loeb, L.B.: The Kinetic Theory of Gases, 3rd edn. Dover Publications, Mineola, New York, (2004)
46. Bird, R.B., Stewart, W.E., Lightfoot, E.N.: Transport Phenomena. Wiley, New York (1960)
47. Perry, W.L., Sewell, T.D., Glover, B.B., Dattelbaum, D.M.: Electromagnetically induced localized ignition in secondary high explosives. J. Appl. Phys. **104**(1), 094906-094906-6 (2008)
48. Cooper, P.W.: Explosives Engineering. Wiley-VCH, New York (1996)
49. Parker, G.R., Asay, B.W., Dickson, P.M., Henson, B.F., Smilowitz, L.B.: In: Shock Compression of Condensed Matter, American Physical Society Topical Conference, Portland, OR, 20–25 July 2003
50. Dickson, P.M.: Private Communication
51. FlexPDE 3. Copyright PDE Solutions Inc., Antioch, CA (2003)
52. Merzhanov, A.G., Dubovitskii, F.I.: Proc. USSR Acad. Sci. **129**, 153–156 (1959)
53. Zeldovich, Y.B., Barenblatt, G.I., Librovich, V.B., Makhviladze, G.M.: The Mathematical Theory of Combustion and Explosions (English Translation) Consultants Bureau, New York, 98–103 (1985)

Springer

http://www.springer.com/978-3-540-87952-7

Shock Wave Science and Technology Reference Library, Vol. 5
Non-Shock Initiation of Explosives
(Ed.)B. Asay
2010, XVII, 617 p. 298 illus., 2 in color., Hardcover
ISBN: 978-3-540-87952-7